

Effective description of the interaction between anisotropic viscous fingers

MICHAŁ PECELEROWICZ, AGNIESZKA BUDEK and PIOTR SZYMCZAK

Institute of Theoretical Physics, Faculty of Physics, University of Warsaw - Hoza 69, 00-618, Warsaw, Poland

received 11 July 2014; accepted in final form 9 September 2014
published online 30 September 2014

PACS 47.20.-k – Flow instabilities
PACS 47.55.-t – Multiphase and stratified flows
PACS 05.45.-a – Nonlinear dynamics and chaos

Abstract – We study patterns formed by viscous fingering in a rectangular network of microfluidic channels. Due to the strong anisotropy of such a system, the emerging patterns have a form of thin needle-like fingers, which interact with each other, competing for an available flow. We develop an upscaled description of this system in which only the fingers are tracked and the effective interactions between them are introduced, mediated through the evolving pressure field. Due to the quasi-2d geometry of the system, this is conveniently accomplished using conformal mapping techniques. A complex two-phase flow problem is thus reduced to a much simpler task of tracking evolving shapes in a 2d complex plane. This description, although simplified, turns out to capture all the key features of the system's dynamics and allows for the effective prediction of the resulting growth patterns.

open access

editor's choice

Copyright © EPLA, 2014

Published by the EPLA under the terms of the Creative Commons Attribution 3.0 License (CC BY). Further distribution of this work must maintain attribution to the author(s) and the published article's title, journal citation, and DOI.

Interfacial instabilities are a driving force of many pattern-forming processes in nature, be it in the realm of fluid mechanics, flame propagation or directional solidification [1–3]. A large body of work has been devoted to the analysis of these processes throughout the last decades. Initial phases of the evolution of an interface are well understood in terms of linear stability analysis, which yields the wavelength of the most unstable perturbation. Much less is known, however, about the nonlinear regime, when the initial perturbations of the interface are transformed into finger-like structures that advance into the system. These nonequilibrium structures interact with each other in a strongly nonlinear way, which gives rise to a complex dynamics of the front, particularly challenging to analyze. For example, in miscible fingering problem [4,5], the emerging fingers are incessantly merging, fading, shielding, and tip splitting [6–8], but no detailed quantitative characterization of this nonlinear dynamics has been provided yet.

In this letter, we consider a particular class of fingered growth systems, in which the emergent fingers are long and thin. Due to the high field gradients at their tips, these structures grow predominantly in length,

but not in diameter. Such structures are observed *e.g.*, in the electrochemical deposition experiments [2,9], wormhole formation in dissolving rocks [10], smoldering combustion [11–13], side-branches growth in crystallization [14,15], or the evolution of seepage channel networks [16,17]. For systems of this kind, we show that the dynamics can be followed using a higher-level description, in which the microscopic details are neglected and the system is treated as a collection of emergent structures—thin lines interacting with each other through a continuous field. The model turns out to be remarkably effective in predicting the evolution of the fingering pattern. Importantly, the complexity of such description decreases with time, as only the longest lines need to be tracked while the shorter, screened ones can be neglected. Thus, somewhat paradoxically, the emergence of structures in such pattern-forming systems can lead to the simplification of the description of the system's dynamics.

We illustrate these ideas with experimental results on anisotropic viscous fingers formed in a network of microfluidic channels. In classical viscous fingering experiments [18,19], such a multi-finger growth regime is just a short transient, and soon the fingers coalesce into a

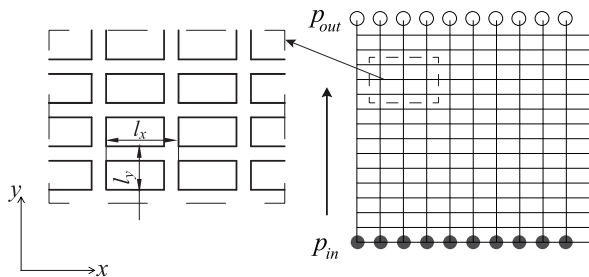


Fig. 1: Schematic of the channel network. The less viscous fluid (water) is injected along the lower boundary into the system initially filled with a more viscous fluid (oil).

single-finger final state. To prevent such a coalescence, we have carried out the viscous fingering experiments in a rectangular grid of channels. In the experimental setup, the microchannel network has been engraved in the polycarbonate plate using a micro milling machine and then bonded with another, flat plate in a thermal press. The details of the bonding procedure are given in [20]. A schematic view of the channel network is presented in fig. 1. The network comprised 42×100 channels with the length of horizontal connectors $l_x = 1200 \mu\text{m}$ and vertical connectors $l_y = 400 \mu\text{m}$. The cross-sections of the channels were $200 \mu\text{m} \times 200 \mu\text{m}$. During the experiments, the network was initially filled with motor oil (of $\mu \approx 500 \times 10^{-3} \text{ (Pa} \cdot \text{s)}$) whereas the invading fluid was water dyed with ink (on the polycarbonate surfaces the oil is wetting with respect to water). The mean velocity of fluids in tubes was around $14 \times 10^{-3} \text{ (m/s)}$. The interfacial tension between water and oil was assumed to be around $15 \times 10^{-3} \text{ (N/m)}$ which corresponds to the capillary number $\text{Ca} \simeq 0.5$. More details of the experimental procedure together with a comprehensive analysis of the patterns obtained in this and similar experiments will be given a forthcoming publication [21].

The displacement of oil by water in our experimental system led to the emergence of elongated, straight dendrite-like fingers, the examples of which are presented in fig. 2. Initially, many small fingers appear, with lengths controlled by the random noise. Subsequently, however, the dynamics becomes deterministic, with longer fingers screening the shorter ones and a hierarchical structure of fingers is formed. It is in this regime that the higher-level model of the finger growth can be introduced.

Let us briefly describe the key steps involved in the construction of the model. We start from the description of the dynamics at the microscopic level, which here corresponds to resolving the flow in individual channels. Assuming that the pressure drop in the invading low-viscosity fluid is negligible, we are only left with the task of computing the pressure field in the displaced fluid. To this end we combine the continuity condition

$$\sum_i q_{ij} = 0, \quad (1)$$

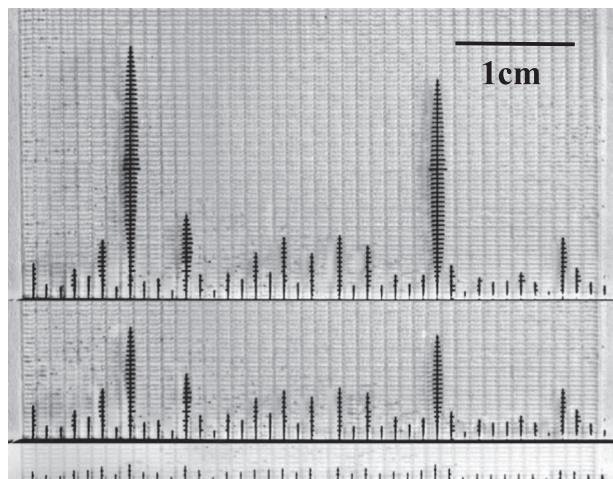


Fig. 2: Evolution of the patterns in the viscous fingering experiment. The patterns are captured at different time points. The invading fluid (water) is dyed with ink, hence the dark color. Successive frames correspond to the situation after 0.5 s, 1 s and 1.8 s after the start of water injection.

with the Poiseuille equation for the volumetric flux

$$q_{ij} = -\frac{p_j - p_i}{\rho l_{ij}}, \quad (2)$$

where $(p_j - p_i)$ denotes the pressure drop along the channel joining node i with node j , q_{ij} is the volumetric flux in this channel, l_{ij} its length and ρ the hydrodynamic resistivity of the channel, involving the fluid viscosity and geometrical characteristics of a capillary. We assume that the finger moves with the velocity corresponding to the mean flow rate in the capillary, *i.e.* $v_i = \frac{q_i}{s}$, where s is the cross-sectional area of the capillary. Together, eqs. (1) and (2) are the hydraulic equivalents of Kirchhoff's circuit rules, and constitute the basic equations of pore-network models of porous media [22]. On scales which are large in comparison with the channel lengths, these equations can be interpreted as a discretization of a continuous anisotropic Laplace equation:

$$\frac{l_x}{l_y} \frac{\partial^2 p}{\partial x^2} + \frac{\partial^2 p}{\partial y^2} = 0, \quad (3)$$

where l_x and l_y are the lengths of the horizontal and vertical channels, respectively (in the experiments reported here, $l_x/l_y = 3$). Rescaling the horizontal coordinate by $x' = \sqrt{l_x/l_y} x$ leads finally to the standard Laplace equation in x', y space.

The next step in the construction of the model is to replace the needle-like fingers by infinitely thin lines interacting through the continuous pressure field, as described by (3). Such thin-finger models have been considered previously in [23–26]; however a direct comparison between a model of this kind and a real experimental system has never been attempted. Another important difference between the above works and the model considered here

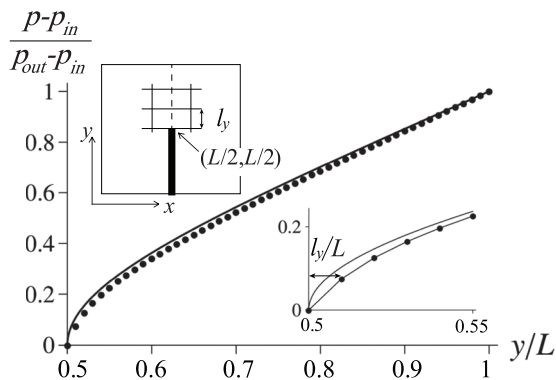


Fig. 3: The pressure field along the centerline of the system (dashed line in the upper inset) with a single finger extending between $(L/2, 0)$ and $(L/2, L/2)$. Solid line: solution of anisotropic Laplace equation (3). Points: pressure calculated based on the Kirchhoff's rules (1), (2). The lower inset shows the neighborhood of the finger's tip.

is that the fingers in [23–26] are allowed to bend to follow the field gradient lines, whereas here—due to the presence of the lattice—they move along the straight lines in the direction of the external pressure gradient. There are several other processes in which such structures are formed spontaneously, *e.g.* side-branch growth in solidifying dendrites or wormhole formation in dissolving porous rock [10,15,27].

However, there is a price to pay for the simplification: since the finger is assumed to be infinitely thin, there is a singularity in a field gradient at its tip. Namely, at a small distance r from the tip of i -th finger, the pressure takes the form

$$p_i(\mathbf{r}, t) = C_i(t)\sqrt{r}\cos(\theta/2), \quad (4)$$

where the coefficients $C_i(t)$ depend on lengths and shapes of all the fingers. In the above, the origin of coordinates is located at the tip of the finger and the polar axis is directed along it. The pressure gradient will then have $r^{-1/2}$ singularity. In the actual experimental system this singularity is removed, since the pressure gradient in each elementary channel comprising the network is approximately constant. This is illustrated in fig. 3, which compares the continuous solution for the pressure field around a thin finger of half the length of the system with the solution of the discrete Kirchhoff's equations (1), (2). As observed, the two solutions agree to a good degree of accuracy. Close to the finger tip, the pressure gradient can thus be approximated by $C_i(t)/\sqrt{l_y}$ and the advancement velocity of the tip is then

$$v_i = \frac{C_i(t)}{\rho s \sqrt{l_y}}. \quad (5)$$

The analysis of the pressure drops in the channels near the finger tip allows us also to explain the fact that the fingers grow straight, without curving. Namely, let us

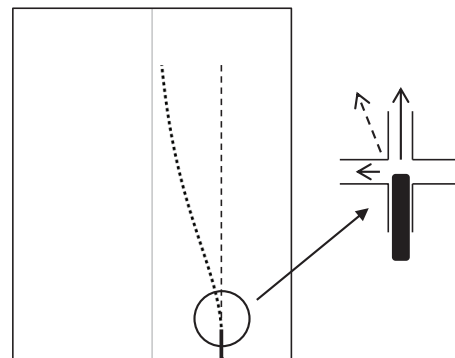


Fig. 4: The growth of a single finger seeded asymmetrically in the 2d system with reflecting walls. The initial seed is marked by a thick black line; the dotted line marks the evolution of the finger in the continuous system [26], whereas the straight, dashed line shows its evolution in the lattice. The inset shows the magnitudes of the pressure gradients in the channels near the finger tip (solid arrows) and the pressure gradient in the continuous system (dashed arrow), directed at an angle to the vertical.

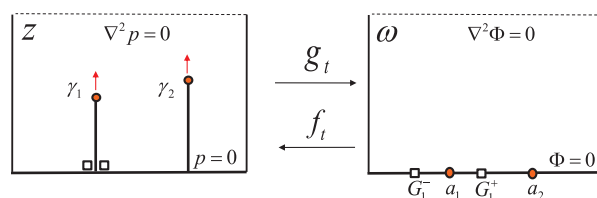


Fig. 5: (Color online) The mapping g_t of the exterior of the fingers onto the empty system (ω -plane). The images of the tips $\gamma_i(t)$ are located on the real line at the points $x = a_i(t)$ (circles). The points G_i are the two pre-images of $\gamma_i(0)$ (squares), *i.e.* $f(G_i^\pm) = \gamma_i(0) \pm \epsilon$.

consider a small “seed” of a finger, positioned off the center axis, as shown in fig. 4. In a continuous system, such a finger will begin to bend towards the centerline of the system [25] (dotted line in fig. 4). In the discrete system, however, the bending is impeded as there are only two possible growth directions: horizontal and vertical. The pressure drop along the former is much smaller than that along the latter, thus the finger continues to grow straight, with just small side-branches produced in the transverse direction, which subsequently get screened off by a faster growing tip.

Because of the quasi-2d geometry of the system, the Laplace equation is conveniently solved by the conformal mapping techniques. To this end, one finds a mapping $g_t(z = x + iy)$ which transforms the region filled with the displaced fluid onto the empty system (ω -plane in fig. 5). The solution of the Laplace equation in the ω -plane is simply $\Phi(\omega) = \text{Im}(\omega)$, which—when transformed back onto the original domain—yields the pressure, $p(z) = \text{Im}(g(z))$. The description of the system in terms of g_t is remarkably convenient, as g_t can be shown to obey a first-order ordinary differential equation

(deterministic Loewner equation), a considerable simplification in comparison to the partial differential equation describing the boundary evolution.

The exact form of the Loewner equation depends on the shape of the domain in which the growth takes place [28,29]. For the growth of thin fingers in the system bounded by reflecting walls, it reads [25]

$$\dot{g}_t(z) = \frac{\pi}{2} \sum_{i=1}^n d_i(t) h(g_t(z), a_i(t)) \quad (6)$$

with

$$h(g_t, a) = \frac{\cos\left(\frac{\pi}{2} g_t\right)}{\sin\left(\frac{\pi}{2} g_t\right) - \sin\left(\frac{\pi}{2} a\right)} \quad (7)$$

and the initial condition $g_0(z) = z$ corresponding to the empty space with no fingers. Note that the poles of the RHS of eq. (6) are located at the images of the tips, $a_i(t) = g_t(\gamma_i)$ (cf. fig. 5). The functions $d_i(t)$ are the so-called growth factors, controlling the speed with which the fingers are growing. By Taylor expanding the inverse mapping, $f_t = g_t^{-1}$ around $a_i(t)$, the exact relation between $d_i(t)$ and $v_i(t)$ can be shown to be [24,25] $d_i(t) = v_i(t)/|f_t''(a_i(t))|$. On the other hand, the field amplitudes $C_i(t)$ in (4) can also be expressed in terms of the conformal mapping f_t [25] as $C_i(t) = \sqrt{2/|f_t''(a_i(t))|}$. Hence, for the Laplacian growth, with velocities of the fingers proportional to pressure gradients at their tips, the growth factors are expressed as

$$d_i(t) = \frac{1}{\rho s} \sqrt{\frac{2}{l_y}} |f_t''(a_i(t))|^{-3/2}. \quad (8)$$

On the other hand, the pole positions, $a_i(t)$, in the Loewner equation (6) control the shape of the growing fingers. In general it is impossible to find analytically the functional form of $a_i(t)$ which would produce the fingers of a given shape, although efficient numerical methods exist [30]. However, a recent work of Tsai [31] provides a general theoretical framework to find $a_i(t)$ for a large class of finger shapes. In particular, applying these ideas to the case of straight fingers one finds the following set of equations for the evolution of $a_i(t)$:

$$\begin{aligned} \dot{a}_j(t) = & -\frac{\pi}{4} d_j \tan\left(\frac{\pi}{2} a_j\right) + \frac{\pi}{2} \sum_{i \neq j} (d_i + d_j) h(a_j, a_i) \\ & - \frac{\pi}{4} \sum_i d_j (h(a_j, G_i^-) + h(a_j, G_i^+)) \end{aligned} \quad (9)$$

which guarantees that the fingers continue to grow vertically. In the above, G_i^+ and G_i^- are the two pre-images under f_t of the points $\gamma_i(t=0)$, where the fingers start to grow, *i.e.* $G_i^\pm = \lim_{\epsilon \rightarrow 0} g_t(\gamma_i(0) \pm \epsilon)$ (cf. fig. 5). In principle they can be found once the mapping g_t is known but in practice it is more convenient to track their evolution in time using directly (6), *i.e.*

$$\dot{G}_j^\pm(t) = \frac{\pi}{2} \sum_i d_i(t) h(G_j^\pm, a_i). \quad (10)$$

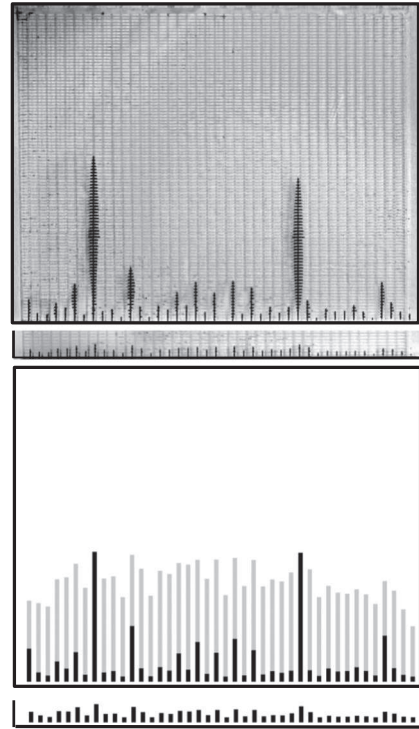


Fig. 6: The comparison of the experimental pattern (top panel) and the one obtained based on the conformal mapping approach (bottom panel) for the same initial geometry, reproduced in a narrow strip below each panel. Black lines correspond to the interacting fingers, whereas gray lines correspond to the case in which the fingers are grown independently.

Together, eqs. (6)–(10) completely determine the evolution of the fingers. Note that this is not just a simple recasting of the problem in terms of another formalism. First of all, the new description is considerably simpler—the entire information about the system is now encoded in the set of finger tips’ positions: γ_i . The dynamics is much simpler to track as well—instead of the original PDE for the movement of the front we now need to deal with $2N + 1$ coupled ODEs (eqs. (6), (9) and (10)). Finally, as will be discussed below, a considerable advantage of this description is the possibility of its further simplification as the front evolves.

The above model is remarkably effective in predicting the dynamics of the fingers, which can be shown by comparing its predictions with the viscous fingering experiment. As mentioned, the initial stages of the finger evolution are noise-driven, which makes them unpredictable except in a statistical sense. However, as soon as the fingers reach the height of a few l_y , the dynamics becomes deterministic, as can be demonstrated by the following procedure: We take the first frame in fig. 2 and approximate the fingers there by a set of line segments of corresponding lengths. Such a configuration is then used as the initial geometry for the conformal mapping solver and the corresponding conformal map g_0 is found. Then, the mapping is evolved according to eqs. (6)–(10). Figure 6 shows the comparison of the pattern produced by

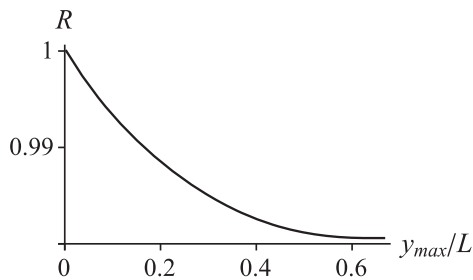


Fig. 7: The Pearson correlation between the two patterns as a function of time (here measured in terms of the length of the longest finger, y_{max}).

such a method with the original experimental pattern. As observed, not only a general, hierarchical structure of the fingers is faithfully reproduced, but even the lengths of individual fingers are in a very good agreement between the model and experiment. This is further confirmed by computing the Pearson correlation between the experimental and theoretical finger lengths as a function of time. As shown in fig. 7, over the entire evolution the correlation between the experiment and the model remains high with the correlation coefficient in the range 0.98–1.

An attractive feature of our model is that the description of the dynamics becomes simpler with time, even though the interface between the two phases gets progressively more rugged in the course of the evolution. To explain this seemingly contradictory observation, let us refer back to fig. 2 and observe that as time progresses, most of the fingers stop to grow and only a few continue to advance through the system. This is caused by a strong, exponential screening between the fingers [25,32,33]: if a shorter finger of length l_1 is positioned between two longer fingers of length l_2 , then the ratio of the field at their tips scales like $e^{-2\pi(l_2-l_1)/a}$, where a is the horizontal distance between them. The speed of the shorter finger will then quickly drop, whereas the longer fingers continue to grow, focusing an ever-increasing portion of the flow. The process is then repeated at a larger scale which leads to the emergence of a self-affine, hierarchical structure. To show that the interaction between the fingers is indeed a crucial factor shaping their evolution, we have included in fig. 6 the pattern in which the fingers are grown independently of each other (gray lines in the figure). Such an “independent” evolution is obtained by running N single-finger problems, where each time just one finger is evolved in an empty system (from a given initial condition) and the influence of others is neglected. As one can see there are dramatic differences between such case and the case of interacting fingers —in the latter, due to the exponential screening, the competition between the fingers is very strong, with a complete stopping of the growth of the shorter ones. In the former (“independent growth”) case all of the fingers continue to grow, albeit with slightly different velocities, since the fingers which were initially longer will always have a larger pressure gradient at their tips than the shorter ones. However, there is no screening

between the fingers in this case and the hierarchical structure does not appear.

The fact that the number of active fingers decreases is crucial from the practical perspective. The growth factors of these fingers become exponentially small, hence they can be removed from the summations (6), (9) and (10), which considerably simplifies the system. For example, in the configuration shown in fig. 6, the velocity of the third longest finger is already more than 20 times smaller than that of the two leading fingers, thus the system effectively becomes a two-body one. In practice, we eliminate the slow fingers from the computations whenever their velocity reaches 10^{-3} of that of the longest finger. When comparing the results of such a procedure with the case in which all of the fingers are tracked, we find differences in finger lengths of less than 0.1%.

Importantly, the method presented here is not limited to the relatively simple fluid displacement problems, but can also be used in the more complicated pattern-forming systems, provided that the following requirements are fulfilled: 1) the patterns should consist of long-and-thin fingers growing predominantly at their tips; 2) the interaction between these fingers is mediated through a certain Laplacian field Ψ (pressure, temperature, concentration, etc.); 3) the velocity of the growth of a single finger is a function or a functional of Ψ and possibly some other, local fields, which are non-zero only within the finger (*e.g.* the reactant concentration field in the problem of chemical erosion of porous rock surfaces by the inflowing acidic solution [10,27,34,35]). In principle, one could also relax the assumption of a Laplacian nature of the field driving the growth, as long as it is conformally invariant. A large class of conformally invariant, non-Laplacian growth processes was identified by Bazant in [36,37] and involves such phenomena as nonlinear diffusion or advection or electromigration coupled to diffusion. One can also generalize the present approach to other different geometries, *e.g.* radial, annular or cylindrical, for which the respective Loewner equation has been derived [25,29,38].

In summary, we have proposed an effective description of the dynamics of anisotropic viscous fingers in terms of thin lines growing at their tips and interacting through the Laplacian pressure field. The model is capable of predicting the final finger pattern in a very accurate way, given the initial “seeds” (*i.e.* the position and lengths of the fingers at the early stage of the evolution, just after the instability). Importantly, the complexity of such description decreases with time, as only the longest fingers need to be tracked while the shorter, screened ones can be removed from the dynamics.

This work was supported by the National Science Centre (Poland) under research Grant No. 2012/07/E/ST3/01734. AB acknowledges the support of the Foundation for Polish Science (FNP) through TEAM 2010-6/2 project co-financed by the EU European

Regional Development Fund. The experiments on viscous fingering in microfluidic channels were conducted together with PIOTR GARSTECKI and ADAM SAMBORSKI from the Institute of Physical Chemistry, Polish Academy of Sciences, who are gratefully acknowledged.

REFERENCES

- [1] PELCÉ P., *New Visions On Form And Growth: Fingering Growth, Dendrites, And Flames* (Oxford University Press) 2004.
- [2] MEAKIN P., *Fractals, Scaling and Growth Far From Equilibrium* (Cambridge University Press) 1998.
- [3] CHARRU F. and DE FORCRAND-MILLARD P., *Hydrodynamic Instabilities* (Cambridge University Press) 2011.
- [4] WOODING R. A., *J. Fluid. Mech.*, **39** (1969) 477.
- [5] HOMSY G., *Annu. Rev. Fluid Mech.*, **19** (1987) 271.
- [6] MENON G., *J. Non-Newtonian Fluid Mech.*, **152** (2008) 113.
- [7] BOOTH R., *J. Fluid Mech.*, **655** (2010) 527.
- [8] ROUSSEAU G., MARTIN M. and DE WIT A., *J. Chromatogr. A*, **1218** (2011) 8353.
- [9] KUHN A. and ARGOUL F., *Phys. Rev. E*, **49** (1994) 4298.
- [10] SZYMCAK P. and LADD A. J. C., *J. Geophys. Res.*, **114** (2009) B06203.
- [11] ZIK O., OLAMI Z. and MOSES E., *Phys. Rev. Lett.*, **81** (1998) 3868.
- [12] ZIK O. and MOSES E., *Phys. Rev. E*, **60** (1999) 518.
- [13] LU C. and YORTSOS Y. C., *Phys. Rev. E*, **72** (2005) 036201.
- [14] COUDER Y., ARGOUL F., ARNÉODO A., MAURER J. and RABAUD M., *Phys. Rev. A*, **42** (1990) 3499.
- [15] COUDER Y., MAURER J., GONZÁLEZ-CINCA R. and HERNÁNDEZ-MACHADO A., *Phys. Rev. E*, **71** (2005) 31602.
- [16] DEVAUCHELLE O., PETROFF A. P., SEYBOLD H. F. and ROTHMAN D. H., *Proc. Natl. Acad. Sci. U.S.A.*, **109** (2012) 20832.
- [17] PETROFF A. P., DEVAUCHELLE O., SEYBOLD H. and ROTHMAN D. H., *Philos. Trans. R. Soc. London, Ser. A*, **371** (2013) 20120365.
- [18] SAFFMAN P. G. and TAYLOR G., *Philos. Trans. R. Soc. London, Ser. A*, **245** (1958) 312.
- [19] KESSLER D. A. and LEVINE H., *Phys. Rev. A*, **33** (1986) 3625.
- [20] OGONCZYK D., WĘGRZYN J., JANKOWSKI P., DABROWSKI B. and GARSTECKI P., *Lab Chip*, **10** (2010) 1324.
- [21] BUDEK A., GARSTECKI P., SAMBORSKI A. and SZYMCAK P., submitted to *J. Fluid. Mech.* (2014).
- [22] BLUNT M. J., *Curr. Opin. Colloid Interface Sci.*, **6** (2001) 197.
- [23] SELANDER G., *Two deterministic growth models related to diffusion-limited aggregation*, PhD Thesis, Department of Mathematics, Royal Institute of Technology, Stockholm, Sweden (1999).
- [24] CARLESON L. and MAKAROV N., *J. Anal. Math.*, **87** (2002) 103.
- [25] GUBIEC T. and SZYMCAK P., *Phys. Rev. E*, **77** (2008) 041602.
- [26] DURÁN M. A. and VASCONCELOS G. L., *Phys. Rev. E*, **84** (2011) 051602.
- [27] COHEN C., DING D., QUINTARD M. and BAZIN B., *Chem. Eng. Sci.*, **63** (2008) 3088.
- [28] LAWLER G. F., *Conformally Invariant Processes in the Plane* (American Mathematical Society) 2005.
- [29] BAUER M. and BERNARD D., *Phys. Rep.*, **432** (2006) 115.
- [30] MARSHALL D. E. and ROHDE S., *SIAM J. Numer. Anal.*, **45** (2007) 2577.
- [31] TSAI J., *J. Math. Anal. Appl.*, **360** (2009) 561.
- [32] EVERTSZ C. J. G., JONES P. W. and MANDELBROT B. B., *J. Phys. A*, **24** (1991) 1889.
- [33] PECELEROWICZ M., BUDEK A. and SZYMCAK P., *Eur. Phys. J. ST*, **223** (2014) 1895.
- [34] DACCORD G., *Phys. Rev. Lett.*, **58** (1987) 479.
- [35] DACCORD G. and LENORMAND R., *Nature*, **325** (1987) 41.
- [36] BAZANT M. Z., CHOI J. and DAVIDOVITCH B., *Phys. Rev. Lett.*, **91** (2003) 045503.
- [37] BAZANT M. Z., *Philos. Trans. R. Soc. London, Ser. A*, **460** (2004) 1433.
- [38] ZHAN D., *Probab. Theory Relat. Fields*, **129** (2004) 340.